Reconciling Past and Future Rainfall Trends over East Africa

DAVID P. ROWELL AND BEN B. B. BOOTH

Met Office Hadley Centre, Exeter, United Kingdom

SHARON E. NICHOLSON

Department of Meteorology, The Florida State University, Tallahassee, Florida

PETER GOOD

Met Office Hadley Centre, Exeter, United Kingdom

(Manuscript received 17 February 2015, in final form 9 September 2015)

ABSTRACT

The ''long rains'' season of East Africa has recently experienced a series of devastating droughts, whereas the majority of climate models predict increasing rainfall for the coming decades. This has been termed the East African climate paradox and has implications for developing viable adaptation policies. A logical framework is adopted that leads to six key hypotheses that could explain this paradox. The first hypothesis that the recent observed trend is due to poor quality data is promptly rejected. An initial judgment on the second hypothesis that the projected trend is founded on poor modeling is beyond the scope of a single study. Analysis of a natural variability hypothesis suggests this is unlikely to have been the dominant driver of recent droughts, although it may have contributed. The next two hypotheses explore whether the balance between competing forcings could be changing. Regarding the possibility that the past trend could be due to changing anthropogenic aerosol emissions, the results of sensitivity experiments are highly model dependent, but some show a significant impact on the patterns of tropical SST trends, aspects of which likely caused the recent long rains droughts. Further experiments suggest land-use changes are unlikely to have caused the recent droughts. The last hypothesis that the response to CO_2 emissions is nonlinear explains no more than 10% of the contrast between recent and projected trends. In conclusion, it is recommended that research priorities now focus on providing a process-based expert judgment of the reliability of East Africa projections, improving the modeling of aerosol impacts on rainfall, and better understanding the relevant natural variability.

1. Introduction

It is well known that East Africa has recently experienced a series of devastating droughts leading to famine and population displacement affecting millions of people. For the ''long rains'' season [March–May (MAM)], these are a manifestation of a long-term decline in rainfall totals (Lyon and DeWitt 2012; Viste et al. 2013; Liebmann et al. 2014). There has been no such downward trend in the ''short rains'' [October–December (OND)], but this season has continued to exhibit large year-to-year variability, which at times has exacerbated the impact of the long rains decline.[1] In contrast, looking ahead to the coming decades, the majority of climate models predict a notable increase in East African rainfall (Shongwe et al. 2011; Otieno and Anyah 2013b; Kent et al. 2015). This disparity has sometimes been called the East African climate paradox and is starkly illustrated in Fig. 1 (drawn to highlight the contrasting decadal trends, which alternatively

Denotes Open Access content.

Corresponding author address: David P Rowell, Met Office Hadley Centre, Fitzroy Road, Exeter EX1 2NX, United Kingdom. E-mail: dave.rowell@metoffice.gov.uk

DOI: 10.1175/JCLI-D-15-0140.1

[1] For simplicity, we adopt the Kenyan terminology for the East Africa's two rainfall seasons. Alternatively, MAM is known as ''belg'' in Ethiopia and ''gu'' in southern Somalia, while OND is known as ''keremt'' in southern Ethiopia and ''deyr'' in southern Somalia.

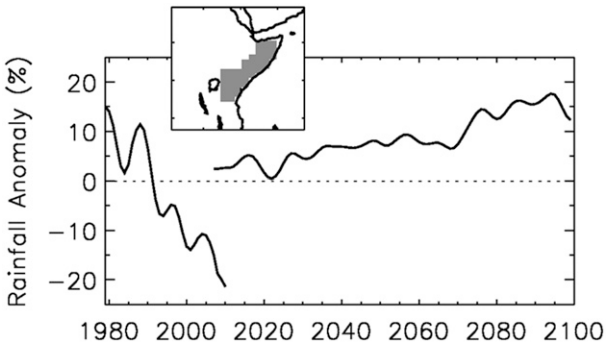

FIG. 1. Lowpass-filtered time series (50% amplitude cutoff at 10 yr) of observed (left-hand line) and projected (right-hand line) MAM rainfall anomalies averaged over the greater Horn of Africa (area shown by inset). Observed data are averaged over seven gridded datasets (section 3a), and projected data are averaged over 39 CMIP5 models forced by the RCP8.5 scenario (Table 1). Units are percentage of the 1901–2000 climatology, calculated using gridded observed datasets available for each year or corresponding CMIP5 historical runs.

can be viewed as evolving probabilities of individual drought seasons).

This raises some important questions. Some have suggested that this contrast between past and future trends throws considerable doubt on the reliability of model projections for the region (Williams and Funk 2011). Alternatively, if the projections can be trusted, others are asking just when we might expect the sequence of drought years to turn to more abundant rainfall and perhaps more frequent flooding [one of three key questions identified by the science plan of the international Hydroclimate Project for Lake Victoria Basin (HYVIC) of the Global Energy and Water Cycle Experiment (GEWEX) project (F. H. M. Semazzi 2015, personal communication)]. These issues are critical to East African livelihoods with an urgent need to develop viable adaptation policies in the face of these disparate threats of food insecurity or flooding. This study therefore addresses these questions by examining a wide range of possible explanations for this apparent contradiction in trends.

Studies to date have primarily focused on the drivers of the recent downward trend of the long rains, with little detailed analysis of the projections. There is general agreement that the rainfall decline is primarily derived from evolving patterns of anomalous SSTs. At interannual time scales, however, the response of the long rains to SSTs is known to be rather weak, particularly in comparison to the short rains (e.g., Ogallo et al. 1988; Camberlin and Philippon 2002). Although this weak interannual link is somewhat ameliorated at decadal time scales as a result of larger signal-to-noise ratios, it nevertheless hampers attribution of the long rains decline to specific SST patterns. Thus, Williams and Funk (2011) believe the Indian Ocean to be the dominant driver, whereas Lyon and DeWitt (2012), Lyon (2014), and Yang et al. (2014) suggest that a pattern reminiscent of La Niña is of prime importance. Within this latter pattern, Hoell and Funk (2014) emphasize the role of the Indo–western Pacific warm pool and Liebmann et al. (2014) emphasize the SST gradient from Indonesia to the central Pacific (identified by Hoell and Funk 2013).

The more important question, however, within the context of the East African paradox, is to ask what has driven these recent SST trends. In particular, are they derived from the natural variability of the climate system or from anthropogenic forcing? Williams and Funk (2011) cite evidence that the Indian Ocean warming (which they believe to be the dominant driver of the rainfall decline) is due to anthropogenic emissions of well-mixed greenhouse gases (WMGHGs). Lott et al. (2013) apply an ''event attribution'' technique to the 2011 long rains drought, concluding that human influence has enhanced the probability of rainfall anomalies at least as dry as that of 2011. Their study did not however extend to determining whether the most relevant anthropogenic forcing was the rise in WMGHGs or changes in aerosol emissions or land use. Similarly, Liebmann et al. (2014) suggest that the relevant warming is due to a combination of ''long-term climate change and natural decadal variability.'' Lyon (2014) and Yang et al. (2014) found, on the other hand, that the evolutions of MAM rainfall and Pacific SSTs differ substantially from the evolution of global warming or CO_2 concentrations, leading them to conclude that the long rains decline has been mainly driven by natural decadal variability. We argue, however, that this does not exclude the possibility that anthropogenic aerosol emissions or land-use changes—with their very different patterns of temporal evolution—might instead have driven part of the recent decadal variability.

In this study we do not focus on any single aspect of the past or projected East African rainfall trends. Rather, our approach is a wide-ranging attempt to objectively lay out all underlying hypotheses that may explain this contrast in trends (section 2) and then (where practical) briefly examine each of these in turn. Our primary aim is to help set priorities for further, more detailed research. Some additional context is provided in section 4 (after describing data sources in section 3), through a careful comparison of model and observed trends and further consideration of the role of SSTs. In sections 5–8 we assess and synthesize the observational and model data relevant to each hypothesis, to begin to understand their possible contribution. Section 9 concludes by evaluating the role of each hypothesis within the context of the other hypotheses, and so recommends priorities for further research.

2. Hypotheses

We first describe a logical framework that encompasses all conceivable hypotheses to explain why two consecutive trends—in this case the observed and projected trends of East African rainfall—could be of differing signs. We emphasize that the aim at this stage is to include all possibilities regardless of preconceptions as to their likelihood. We organize this framework into three overarching ideas: errors in the observed and/or model data, random variability in the climate system, and physical explanations for gradient changes in the decadal evolution of the long rains. These are then subdivided into the six hypotheses addressed through the remainder of the paper.

First, the contrasting rainfall trends may arise from data errors.

- Hypothesis A is that the recent observed trend could be due to poor quality observational data (e.g., poor spatial coverage of rain gauge data or poor interpretation of satellite information), in contrast to a more reliable projected trend.
- Hypothesis B is that the projected trend might be an artifact of poor representation by some key physical processes of the climate models, in contrast to a reliable, and perhaps anthropogenically forced, recent rainfall trend.

The second overarching idea is that either the past or projected trends may arise simply from random sampling of a statistically stable climate.

- Hypothesis C is that the past and/or future trends might arise from natural variability. These variations could be derived from a white noise process, within which a random series of events induces an apparent trend in the data. Alternatively, within a red noise process, the timing of a strong natural multidecadal coupled ocean–atmosphere mode may produce random trends for a period of a decade or more.

Third, there could be genuine physical reasons for the contrast in trends.

- Hypotheses D and E are that the balance between competing anthropogenic forcings could be changing. In particular, the past trend may have been driven more by aerosol emissions (hypothesis D) or by land-use changes (hypothesis E), whereas the projected trend is driven more by carbon emissions.
- Hypothesis F is that the balance between competing mechanisms that determine the response to the dominant anthropogenic forcing could be changing. Alternatively, one or more of these mechanisms may be responding in a nonlinear fashion to this forcing.

Last, a combination of some of these hypotheses may explain the contrast between past and projected rainfall trends.

As noted above, the outcome of assessing these hypotheses has important implications for developing adaptation policies for the region. If research shows that hypothesis B is likely valid (either uniquely or in combination with other hypotheses), then decision-makers must plan for a deeply uncertain future that includes both food insecurity and more frequent flooding. On the other hand, if one or more of hypotheses A, C, D, E, or F is valid, with hypothesis B rejected, then a measured degree of trust in climate model projections can be retained. In this case, decision-makers need account for a more limited range of climate scenarios, potentially leading to more robust decisions, despite a remaining—but reduced—risk of divergent impacts.

Hypotheses C–F are examined in detail in sections 5–8. We will not however examine the first two hypotheses any further. Regarding hypothesis A, there is very good evidence that there has indeed been a recent downward trend in rainfall during the long rains (e.g., Lyon and DeWitt 2012; Viste et al. 2013), along with its sometimes devastating consequences (e.g., Hillbruner and Moloney 2012; Mason et al. 2012). Regarding hypothesis B—that the models' future trends cannot be trusted—we believe that further research on this topic is essential if it is to be confidently refuted or accepted. However, this will likely take several years of effort: first to reach an adequate understanding of the models' mechanisms for this regional upward trend and then to validate the key processes against observational data. So at this stage, we take the pragmatic approach of suggesting that this hypothesis can only be considered likely if initial analysis of all other hypotheses suggests that they explain little of the contrast between observed and projected trends. We also recognize that this judgment depends on one's inherent faith in the capability of state-of-the-art climate models.

3. Data and methods

a. Observed data

We necessarily employ gridded rainfall data, in part to enable comparison with model data, and in part to avoid biasing area averages toward regions of greater gauge density. There are many such gridded reconstructions, each with their own error characteristics. So to account for this variety, we use an ensemble of seven gridded datasets of monthly mean rainfall, as follows.

Four datasets are founded only on rain gauge data: Climatic Research Unit (CRU) Time Series (TS) version 3.21mozfix [CRU TS3.21mozfix, on a 0.5° grid, January 1901–December 2011, an interim version provided by

I. Harris et al. (2014, unpublished data), methods described by Harris et al. (2014)], Global Precipitation Climatology Centre version 4 [GPCC-Reanalysis v4, on a 1° grid, January 1901–December 2007 (Schneider et al. 2011, 2014; noting that reanalysis does not imply use of a physical model)], GPCC-Monitoring [on a 1° grid, January 1986–October 2010 (Schneider et al. 2011, 2014)], and University of Delaware version 2.01 [U.Delaware v2.01, on a 0.5° grid, January 1900–December 2008 (Matsuura and Willmott 2009)]. These datasets differ in the stations they incorporate, and hence their spatiotemporal homogeneity, especially during the last two to three decades, although all include Nicholson's archive of African data (e.g., Nicholson 2015) until at least the 1980s. They also differ in their quality control of this station data, their techniques for filling data-sparse regions and missing months, and their gridding techniques. Furthermore, we note that the number of African stations in at least the CRU dataset declines sharply during the 1990s (Rowell 2013; Harris et al. 2014), and that GPCC-Monitoring relies primarily on data transmitted in quasi real time via the Global Telecommunications System whereas GPCC-Reanalysis incorporates a larger network of stations received through agreements with individual countries. Tanarhte et al. (2012) and Trenberth et al. (2014) provide further discussion.

The other three gridded datasets are merged analyses of rain gauge and satellite data. These have the obvious advantage of more reliable estimates in data-sparse regions, but the disadvantages of more limited temporal duration (all begin in January 1979) and of reliance on the accuracy of the algorithms that convert satellite radiances to rainfall estimates. They are Climate Anomaly Monitoring System (CAMS) outgoing longwave radiation (OLR) precipitation index (CAMS-OPI; Janowiak and Xie 1999a,b), Climate Prediction Center (CPC) Merged Analysis of Precipitation (CMAP; Xie and Arkin 1997a,b), and Global Precipitation Climatology Project version 2.2 (GPCP v2.2; Adler et al. 2003a,b). All are available on a 2.5° grid and extend to December 2011, November 2011, and December 2010, respectively, at the time of download. Note that we include CAMS-OPI for consistency with Lyon and DeWitt's (2012) study of the recent East African rainfall decline, even though Janowiak and Xie (1999a) state that "we strongly suggest the use of the GPCP or CMAP estimates for purposes other than real-time precipitation monitoring on climatic spatial scales."

Additionally, a gauge-based ungridded rainfall dataset (S. E. Nicholson 2014, unpublished data) is used in section 5b to examine historical variations from the late nineteenth century.

Last, the observed SST dataset we employ is the Hadley Centre Sea Ice and Sea Surface Temperature dataset version 1.1 (HadISST1.1) reconstruction of monthly mean SSTs, described by Rayner et al. (2002, 2003). These are available on a 1° grid from 1870 to 2012.

b. Model data

The model data are sourced from phase 5 of the Coupled Model Intercomparison Project (CMIP5; CMIP5 Modelling Groups 2011; Taylor et al. 2012). Our focus is primarily on the past performance and future projections of coupled atmosphere–ocean general circulation models (AOGCMs). Data from three experiments are analyzed: the historical run that simulates climate variability from the mid-nineteenth century to the early twenty-first century and is driven by realistic anthropogenic and natural forcings, the preindustrial control (piControl) run in which all external forcing is fixed at preindustrial conditions (used only in section 5), and the representative concentration pathway 8.5 (RCP8.5) projection of climate change to the late twenty-first century, which is a high-emissions scenario [and therefore most consistent with current emission trends that "track the high end of the latest generation of emission scenarios" (Friedlingstein et al. 2014, p. 709)]. The models used in this study are listed in Table 1, which are those available for download in January 2014.[2] For each model, an initial condition ensemble of historical simulations is available, and a single control experiment (of length recorded in Table 1). The first member of each model's RCP8.5 ensemble is used, since intraensemble variability is small (section 5c) and ensemble size is inconsistent across the models. Additional aerosol and land-use sensitivity experiments are described in sections 6 and 7.

For some of the analysis of past rainfall trends in section 4 we also include data from atmosphere-only GCM simulations (AGCMs). These are the Atmosphere Model Intercomparison Project (AMIP) experiments from CMIP5, which are driven by observed global SSTs and atmospheric constituents. Again, the models used are those available for download in January 2014, and are listed in Table 1, along with the size of the initial-condition ensemble available.

c. Analysis region and period

Much of the following analysis requires area averages of East African rainfall, which ideally would focus on the region of contrasting past and future MAM rainfall

[2] Note that gaps appear in Table 1 where an experiment was not run or, on occasion, data-processing problems were encountered or the experiment ended prematurely. The latter problem also occasionally reduces the ensemble size compared to that theoretically available.

TABLE 1. CMIP5 model experiment details. (Expansions of acronyms are available online at http://www.ametsoc.org/PubsAcronymList.)

Institution, country	Model name	piControl (yr)	Ensemble size		RCP8.5 availability
			Historical	AMIP	
CSIRO–BoM, Australia	ACCESS1.0	249	1	1	√
CSIRO–BoM, Australia	ACCESS1.3	499	1	1	√
BCC, China	BCC_CSM1.1	499	3	3	√
BCC, China	BCC_CSM1.1(m)	399	3	3	√
Bejing Normal University (BNU) College of Global Change and Earth System Science (GCESS), China	BNU-ESM	558	1	1	√
CCCma, Canada	CanAM4	—	—	1	—
CCCma, Canada	CanCM4	—	10	—	—
CCCma, Canada	CanESM2	995	5	—	√
NCAR, United States	CCSM4	500	6	6	√
National Science Foundation (NSF)–DOE–NCAR, United States	CESM1(BGC)	499	1	—	√
NSF–DOE–NCAR, United States	CESM1(CAM5)	318	3	—	√
NSF–DOE–NCAR, United States	CESM1 (FASTCHEM)	221	3	—	—
NSF–DOE–NCAR, United States	CESM1(WACCM)	199	4	—	—
CMCC, Italy	CMCC-CESM	276	1	—	√
CMCC, Italy	CMCC-CM	329	1	3	√
CMCC, Italy	CMCC-CMS	499	1	—	√
Centre National de Recherches Météorologiques (CNRM)–Centre Européen de Recherche et de Formation Avancée en Calcul Scientifique (CERFACS), France	CNRM-CM5	809	10	1	√
CNRM–CERFACS, France	CNRM-CM5.2	358	1	—	—
CSIRO–Queensland Climate Change Centre of Excellence (QCCCE), Australia	CSIRO Mk3.6.0	499	5	9	√
Irish Centre for High-End Computing (ICHEC), Ireland	EC-EARTH	—	1	1	√
IAP (LASG), China	FGOALS-g2	699	5	1	√
First Institute of Oceanography (FIO), China	FIO-ESM	799	1	—	√
NOAA/GFDL, United States	GFDL CM2.1	—	9	—	—
NOAA/GFDL, United States	GFDL CM3	499	5	5	√
NOAA/GFDL, United States	GFDL-ESM2G	499	1	—	√
NOAA/GFDL, United States	GFDL-ESM2M	499	1	—	√
NOAA/GFDL, United States	HiRAM-C180	—	—	3	—
NOAA/GFDL, United States	HiRAM-C360	—	—	2	—
NASA GISS, United States	GISS-E2-H	539	6	—	√
NASA GISS, United States	GISS-E2-H-CC	250	1	—	√
NASA GISS, United States	GISS-E2-R	549	6	6	√
NASA GISS, United States	GISS-E2-R-CC	250	1	—	√
Met Office Hadley Centre (MOHC), United Kingdom	HadCM3	—	9	—	—
MOHC, United Kingdom	HadGEM2-A	—	—	1	—
National Institute of Meteorological Research (NIMR)–Korea Meteorological Administration (KMA), South Korea	HadGEM2-AO	699	1	—	√
MOHC, United Kingdom	HadGEM2-CC	240	3	—	√

TABLE 1. (*Continued*)

Institution, country	Model name	piControl (yr)	Ensemble size		RCP8.5 availability
			Historical	AMIP	
MOHC, United Kingdom	HadGEM2-ES	576	4	—	√
INM, Russia	INM-CM4	499	1	1	√
IPSL, France	IPSL-CM5A-LR	999	6	1	√
IPSL, France	IPSL-CM5A-MR	299	3	3	√
IPSL, France	IPSL-CM5B-LR	299	1	1	√
CCSR/National Institute for Environmental Studies (NIES)/JAMSTEC, Japan	MIROC-ESM	530	3	—	√
CCSR/NIES/JAMSTEC, Japan	MIROC-ESM-CHEM	254	1	—	√
CCSR/NIES/JAMSTEC, Japan	MIROC4h	—	3	—	—
CCSR/NIES/JAMSTEC, Japan	MIROC5	669	5	2	√
MPI, Germany	MPI-ESM-LR	999	3	3	√
MPI, Germany	MPI-ESM-MR	999	3	3	√
MPI, Germany	MPI-ESM-P	1155	2	—	—
Meteorological Research Institute (MRI), Japan	MRI-AGCM3.2H	—	—	1	—
MRI, Japan	MRI-AGCM3.2S	—	—	1	—
MRI, Japan	MRI-CGCM3	499	3	3	√
MRI, Japan	MRI-ESM1	—	1	—	—
Norwegian Climate Centre (NCC), Norway	NorESM1-M	500	3	3	√
NCC, Norway	NorESM1-ME	251	1	—	√
Total No. of models (ensemble members)		42	48 (153)	28 (70)	39

trends. However, the area of recent downward trend varies among observational datasets (not shown), although it commonly extends from Tanzania to southern Ethiopia and westward to at least Lake Victoria. The spatial pattern of the models' projected upward trend is even less consistent. Therefore, neither trend analysis dictates a tailored choice of averaging region. We therefore adopt the greater Horn of Africa region (hereinafter GHAfrica; Fig. 1, inset) defined by Rowell (2013), which encompasses much of Kenya and Somalia along with parts of southeastern Ethiopia and northeastern Tanzania. The observational datasets all exhibit a recent downward trend across this region, apart from considerable uncertainty in northern Somalia. A majority of models also exhibit a projected upward trend over almost the entirety of this region. Furthermore, and importantly from a mechanistic point of view, this region also approximately matches the areas that experience their wettest month during one of the transition seasons (Nicholson 2014). Nevertheless, to assess the sensitivity to this choice of region, results were also repeated with Lyon and DeWitt's (2012) and Yang et al.'s (2014) larger region (which additionally encompasses substantial areas where rainfall peaks during the solstitial months). The conclusions were unaltered by this sensitivity test.

Throughout this study, observed and modeled data have been interpolated onto a common grid for necessity, and the grid chosen to be that of recent Met Office models: 1.25° latitude × 1.875° longitude. The GHAfrica averages were then computed from this regridded data.

The long rains season is defined here as the March–May seasonal average. Much of the following analysis was also repeated by separately stratifying the data for each of the three individual months, but no substantive differences were found from the seasonal analysis, unless otherwise stated.

Last, the observational period on which we primarily focus is 1986–2007; these being the common years of the gridded datasets listed in section 3a, as well as encompassing much of the recent trend. Sensitivity of the trend to this choice was assessed by varying the start and end dates by 1–2 yr and then recomputing the trend. For each dataset, the standard error of the resulting trends is 14%–19% of its 1986–2007 trend, except for the CRU dataset, which has a standard error of 30% as a result of a weaker trend.

4. Rainfall trend characteristics and SST links

Figure 1 presented a motivational illustration of the contrast been recent and projected rainfall trends during the long rains season. Figure 2 now presents more detail, adding information on observational and modeling uncertainties, and the seasonality of these trends. The recent observed drying (Fig. 2a) is clearly a feature unique to the

long rains, and is apparent throughout this season (March–May), with broad agreement between each of the seven gridded datasets. This contrasts with an upward trend during the early part of the short rains and little or no trend in other seasons. Furthermore, the downward trend of the long rains is only a feature of the last 2–3 decades, with no consistent trend through the twentieth century (cf. Figs. 2a and 2c, noting their different scales).

In contrast, the projected upward trend of future rainfall is most apparent when computed for the entire twenty-first century (Fig. 2d), whereas no consensus (or even majority view) exists for the more immediate future (Fig. 2b). This difference in time scale compared to the past may in itself suggest that different forcings or mechanisms could be at play in the past and future long rains trends. Note that, despite the rate of change being substantially weaker for the future than the past (cf. Figs. 2d and 2a), the former is sustained for many more decades, so typical magnitudes of the anomalies may become similar (but with opposite sign). Even so, in a minority of models the rate of rainfall increase is close to the magnitude of change experienced in the recent past. A final feature of Fig. 2d is a strong seasonality in the relative consensus of increasing rainfall, with near unanimity in the boreal winter months (November–April), but substantial uncertainty in the sign of change during the boreal summer months (May–September). Understanding this seasonality is beyond the scope of the current study, but should be an important aspect of future research aimed at addressing the reliability of these projections.

An important question that now follows is whether or not climate models are capable of simulating this recent decline in the abundance of the long rains. The answer could provide further clues about the mechanisms of this past trend, as well as information on the ability of models to respond to any external forcing. Figure 3a illustrates recent bidecadal trends for GHAfrica for all available CMIP5 historical AOGCM simulations (light gray bars). Each model and each observational dataset is scaled by its own interannual standard deviation to ensure a fair comparison. Note that the trend period ends slightly earlier because the simulations only run to 2004 or 2005. A wide variety of trends is simulated, with their distribution centered close to zero. Only a small minority of model runs are able to match the observed downward trend (shown by vertical lines). The darker bars show the spread of results from the two 10-member initial condition ensembles, and it is clear that much of the spread across the entire CMIP5 ensemble arises from random phasing of natural multidecadal variations in the coupled system, as well as from intermodel variability [cf. the single-model ensemble analysis of Liebmann et al. (2014)]. A key question through the remainder of this paper is whether this large natural variability fully accounts for the failure of many models to duplicate the observed trend, or whether many models are also failing to respond to an external forcing.

Figure 3b then illustrates the recent bidecadal long rains rainfall trends for the CMIP5 AMIP simulations (i.e., derived from atmosphere-only models forced by observed SSTs). Again a proportion of the spread is due to random variability, in this case chaotic variations internal to the atmosphere. The remaining spread is due to modeling uncertainty. Critically, however, the distribution of AMIP trends is notably skewed toward negative trends. First, this suggests that the observed downward trend is also at least partly driven by anomalous SST patterns [see also Yang et al.'s (2014) analysis of a subset of CMIP5 AMIP simulations for their larger region]. Second, it demonstrates that most models are able to capture this SST impact on the long rains [cf. also Lyon and DeWitt's (2012) sensitivity experiments], albeit with weaker-than-observed trends, which either reflects some deficiency in most models or the effect of large chaotic atmospheric anomalies in the real world.

Figure 4a shows the observed trend in MAM tropical SSTs from 1986 to 2007, aspects of which are at least partly responsible for the East African rainfall decline (Fig. 3b). Figure 4b then shows the long-term low-frequency (greater than 10 yr) MAM relationship between tropical SSTs and GPCC-Reanalysis GHAfrica rainfall (near-identical results are obtained with CRU or U.Delaware data). An independent period is chosen, 1922–85, beginning when rain gauge density significantly improves (Rowell 2013) although results for 1901–85 are similar. Inevitably, this analysis samples only a few decades, so the interpretation of Fig. 4b should be somewhat tenuous. The pattern of recent cooling in the northeastern tropical Pacific, with warming to the southwest and northwest (Fig. 4a), is consistent with the opposing sign of the eastern Pacific decadal correlation pattern (Fig. 4b) and with the idealized GCM experiments of Lyon and DeWitt (2012), suggesting it to be a prime candidate driver of the East African drying. Most AOGCMs fail to capture this SST pattern, particularly the region of cooling (not shown). In contrast, the weak 1986–2007 warming of the Indian Ocean and its positive twentieth-century decadal correlations appear inconsistent with the East African drying. This suggests either that the Indian Ocean did not contribute to the rainfall decline, or changes in its SST pattern were more influential than its overall warming, or that its relationship with the long rains has been altered, perhaps because of changes in external forcing. In our view, a clear attribution of the recent decline of the long rains to specific SST patterns now requires multimodel idealized SST experiments and a more detailed analysis of the mechanisms involved.

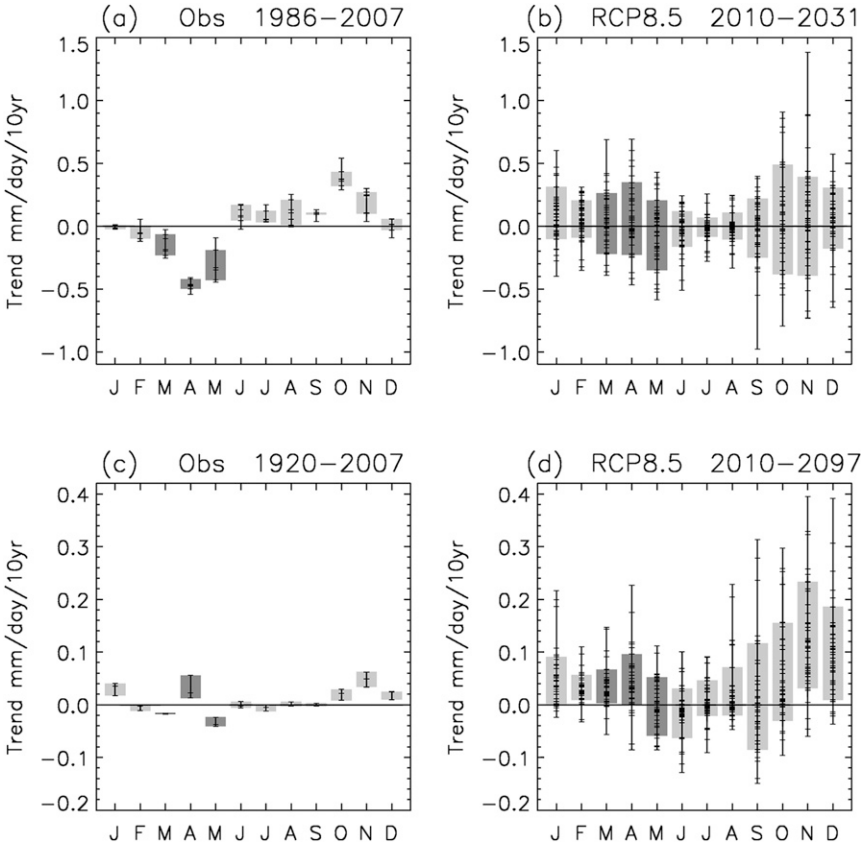

FIG. 2. Annual cycles of (left) observed and (right) projected GHAfrica rainfall trends (mm day^{-1} decade^{-1}) for (a),(b) 22- and (c),(d) 88-yr periods. Tick marks on each vertical line show results for individual datasets or models, and gray bars mark approximately the central 70% of datasets. Dark gray bars highlight the MAM long rains.

To conclude this section, we emphasize the following. The different time scales of past and future trends in Fig. 2 suggest (but do not prove) that different mechanisms or forcings may be driving each of these long rains trends. The distributions of model rainfall trends in Fig. 3 then raise questions that can be framed from two perspectives. From a mechanistic point of view, we can ask what has driven the SST trends that appear to have caused the recent rainfall decline. Are they entirely accounted for by a natural coupled ocean–atmosphere mode, or rather, are they driven by anthropogenic emissions within the context of significant natural variability? Alternatively, from a modeling point of view, we must ask whether the majority of historical runs are poor simply because they inevitably fail to replicate the phasing of the observed natural multidecadal fluctuations, or whether they are missing or poorly representing some key processes. Clearly, these modeling and mechanistic perspectives are interlinked, with progress on each informing the other. The role that natural variations may play in the observed GHAfrica trend will now be isolated.

5. Natural variability (hypothesis C)

Here, we address the hypothesis that the recent and/or future trends in East African MAM rainfall are due to natural variability of the ocean–atmosphere system. Two complementary approaches are taken to examine the role of natural variability in the past climate, before briefly examining its role in future trends.

a. Significance of observed trends against unforced AOGCM variability

The first approach assesses whether or not the recent rainfall trend significantly differs from those found in an unforced climate system. We compare the observed 1986–2007 trend with the range of 22-yr trends from long unforced control runs of CMIP5 coupled models in which anthropogenic forcing (and external natural forcing) are absent. The variability in these integrations, at all time scales, arises only from natural processes, so if they do not sometimes reproduce 22-yr trends of similar magnitude to those observed, then this would suggest

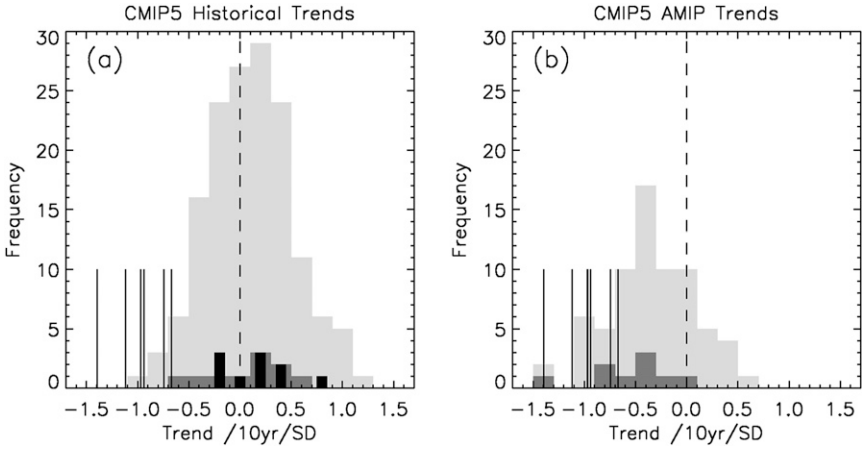

FIG. 3. Histograms of CMIP5-simulated trends of GHAfrica MAM rainfall for (a) historical and (b) AMIP integrations, for 1986–2004. Light gray bars use all available models and ensemble members. Dark gray and black bars use ensemble members for a single model: CNRM-CM5 and CanCM4, respectively, in (a) and CSIRO Mk3.6.0 in (b). Solid vertical lines are trends in the seven observational datasets, for the same periods as the model data. Each model and observed dataset is scaled by its interannual standard deviation.

that hypothesis C should be rejected. The alternative approach of using the standard statistical test for the significance of a trend (e.g., von Storch and Zwiers 1999) is unsuitable because it assumes a white noise process, which could be invalidated here by slow ocean processes. Use of model control simulations to provide a benchmark of unforced trends overcomes this issue. Nevertheless, this analysis does assume the models properly characterize the real world in this regard, so it would be unwise to rely on it as a solitary line of evidence.

For each of the CMIP5 models' preindustrial control runs (Table 1), the trend in GHAfrica MAM rainfall is computed for all 22-yr periods.[3] These are then normalized by the standard deviation of each model's full time series to correct for biases in their total variance. This is necessary because errors in the models' mean rainfall climate often contribute to errors in the total variance (e.g., an underestimate of mean rainfall usually leads to a similar underestimate in variability), and this must be corrected so that our analysis does not simply reflect any systematic biases in the models' mean climate and total variance. This normalization is also applied to the recent 22-yr trends from the seven gridded observational datasets. Thus, we correct for the models' first-order errors in total variance, but necessarily ignore second-order errors in the ratio of decadal-to-interannual variance. We can then assess whether the observed trends differ significantly from those arising from natural processes by computing the percentile at which each of the observed trends lies within each models' distribution of unforced trends. This leads to 7×42 percentiles, which compare the seven observational datasets with each of the 42 models. The distribution of percentiles for each of the seven observed 1986–2007 trends is shown in Fig. 5.

Six of the observed estimates of the long rains trend are significantly different from those due to simulated natural variability alone, assessed against almost all CMIP5 models at the 10% significance level, and against most (or some) models at the 5% level. The exception is the weaker trend of the CRU TS3.21mozfix dataset (also consistent with the CRU TS3.20 dataset trend but less consistent with the CRU TS3.10 trend, which is weaker still). The reason for its different behavior is unclear, although possibilities are listed in section 3a.

In summary, this evidence suggests that the observed rainfall trend is at least very unusual with respect to natural climate variations. However, as stated earlier, this is founded on an assumption that the models' properly represent the decadal component of the rainfall variability. We therefore complement this analysis with a search for observed precedents of persistent long rains drought during the preceding century.

b. *Nineteenth- and twentieth-century precedents for decadal drought*

Nicholson et al. (2012) analyzed a combination of gauge and documentary data to provide an exceptionally

[3] The entire model time series was first detrended to eliminate any long-term drift. The start dates of the 22-yr trend periods were then chosen to be 1 yr apart, noting that the lack of independence between periods has no adverse effect on the analysis, but instead ensures that trends between all multidecadal peaks and troughs are properly sampled.

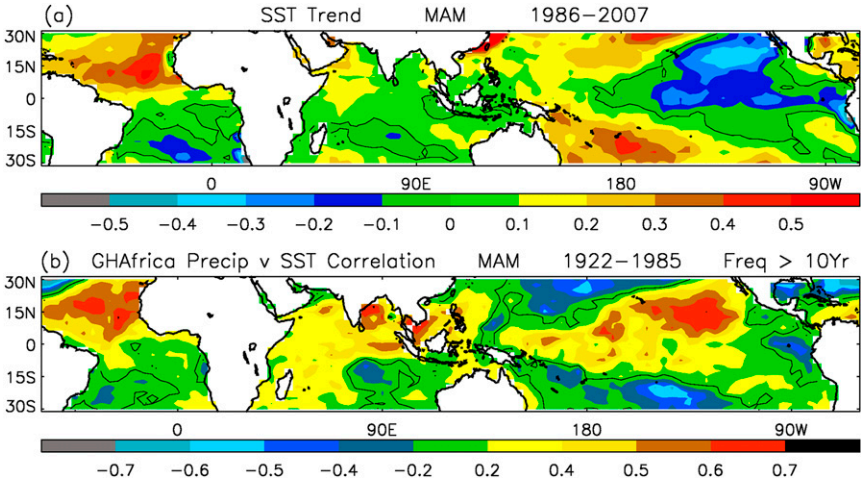

FIG. 4. (a) The 1986–2007 MAM SST trends (°C decade^{-1}). (b) Correlation between GHAfrica MAM rainfall and local MAM SSTs for 1922–85, using lowpass-filtered data with a 50% amplitude cutoff at 10 yr.

long time series (200 yr) of an annual wetness index for five regions of Africa. For East Africa, two precedents for persistent drought were found: 1821–39 and 1879–1902 (although the latter is broken by above average wetness during 1892–95). These are likely caused by natural variations of the climate system, since anthropogenic emissions were relatively low during the nineteenth century, and the timing of volcanic eruptions does not consistently provide an explanation (cf. Gao et al. 2008). This potentially suggests that the current long rains drought could be similarly due to natural variability. However, a limitation of the Nicholson et al. (2012) data, within the context of the current study, is that it provides only annual information. A critical question, therefore, is whether these nineteenth century drought periods have their origin in the long rains, the short rains, or a chance sequence of drought years in a mix of seasons.

Unfortunately, no seasonally stratified information is available for the 1821–39 drought period; so we focus on the late nineteenth century onward, for which some early rain gauge records are available. Data are analyzed for the area shown by the inset in the top panel of Fig. 6, which is identical to that used by, for example, Nicholson (2000) and Nicholson et al. (2012), except that a few stations in far eastern Zaire (now the Democratic Republic of Congo) are excluded because of the sharp decline in data

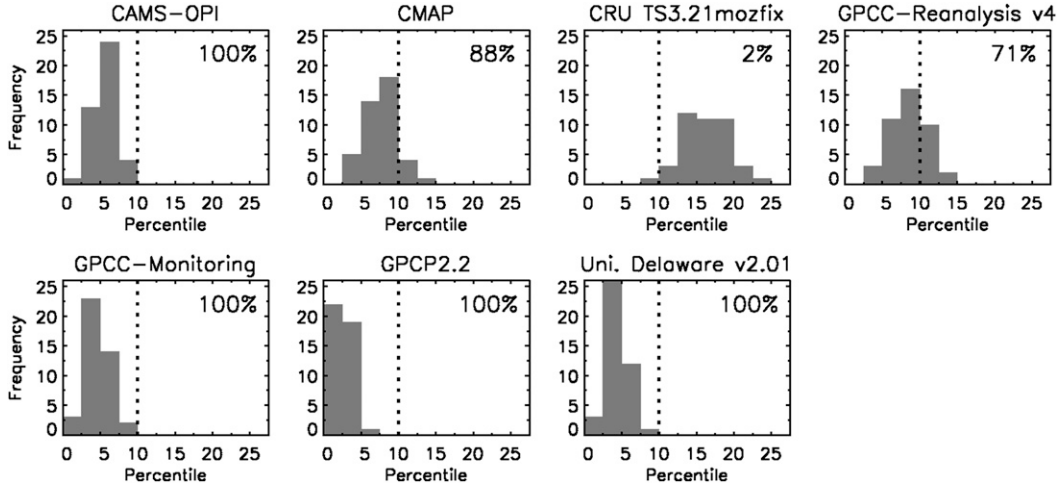

FIG. 5. Histograms of the percentile at which an observed 1986–2007 trend lies within the distribution of unforced 22-yr trends sampled from long CMIP5 control integrations. All trends are for GHAfrica MAM average rainfall, each histogram documents the results for a trend from a single observational dataset, and each model contributes a single percentile to each histogram. The values at the top right of each panel record the percentage of models for which the observed trend lies below the 10th percentile.

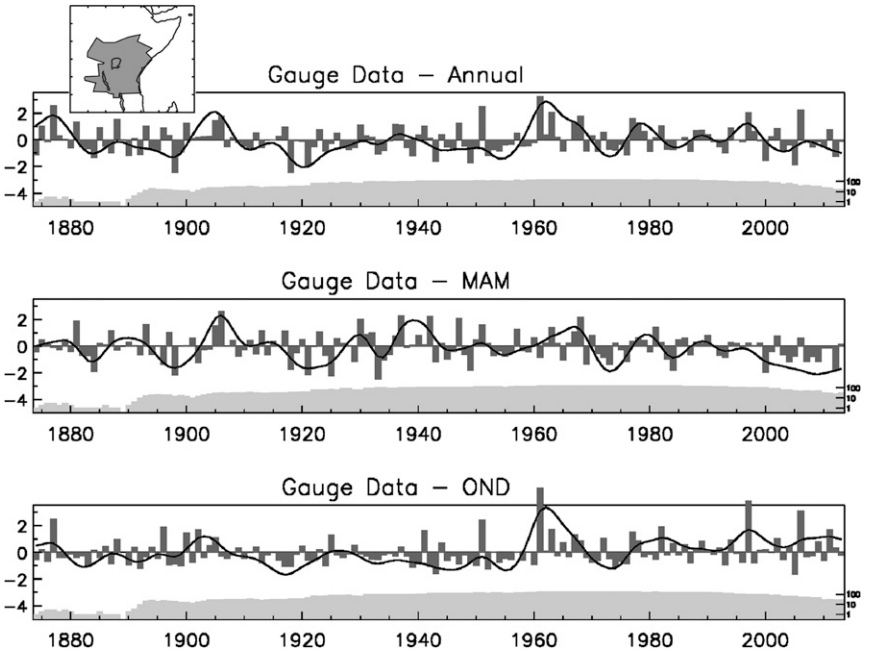

FIG. 6. Standardized time series of East African rainfall (dark gray bars) and lowpass-filtered rainfall (solid line, using 50% amplitude cutoff at 10 yr), computed from gauge data averaged over the region (shown by the inset at top), and using a 1901–2000 baseline: (top) annual means, (middle) MAM means (long rains), and (bottom) OND means (short rains). Light gray bars and right-hand scale show the number of gauges available for each year or season. Note that data are lowpass filtered then standardized

availability from 1984. To construct the time series, rainfall at each station is computed as a departure from the long-term mean divided by its standard deviation, this calculation being stratified by season as appropriate. A simple average over all available stations is then calculated, and so units represent a regionally averaged standard deviation. The resultant time series of annual means exhibits consistent interannual variability with the gridded rainfall datasets used elsewhere in this paper; the gauge time series (Fig. 6, top) correlates at 0.85–0.89 with the CRU, GPCC-Reanalysis, and U.Delaware GHAfrica time series, for 1901–2007 (the shortfall from perfect correlations being due to the change in both dataset and region).

Figure 6 (top) also shows that these gauge records support Nicholson et al.'s (2012) evidence of two decades of annual mean drought at the end of the nineteenth century, although with somewhat reduced intensity and persistence; 1882–99 precipitation exhibits 11 dry years, 4 wet years and 2 near-average years (1889 has no data). However, prior to 1893 this time series is based on relatively few stations (Fig. 6, top). So to confirm the reliability of these nineteenth-century gauge-based averages, we correlate the average of the stations available prior to 1893 (Zanzibar, Tanzania; Kampala, Uganda; and Mombasa, Lamu, and Malindi, Kenya) with the time series based on all stations, using the period 1922–94, which has a relatively complete and constant station network. For the short rains this correlation is 0.86, and even during the long rains (when spatial coherence is lower; e.g., Nicholson 1996; Hastenrath et al. 2011) the correlation is 0.59, still highly statistically significant.

The middle and bottom panels of Fig. 6 then stratify this long-term gauge time series by East Africa's two wet seasons. Neither season exhibits a persistent sequence of droughts, but rather the annual mean 1882–99 droughts are derived from a mix of long rains and short rains droughts. This longer observational record also facilitates a comparison between the recent long rains drought and earlier events. Analysis of the minima of the lowpass-filtered MAM time series shows the recent drought to be the most intense on record: −2.1 standardized units compared to −1.9 in 1973 and −1.7 in 1898 and 1921. Alternatively, by analyzing rolling 10-yr periods, it is also the most persistent on record, with 9 out of 10 years of below average rainfall compared to 7 out of 10 years at the turn of the twentieth century and during the 1950s. Last, a comparison of rolling 22-yr trends shows the recent trend to be exceeded only by the 1904–25 transition from two consecutive wet years to a period with just three intense droughts over seven years. Thus, this long observational record shows the current period of long rains drought is

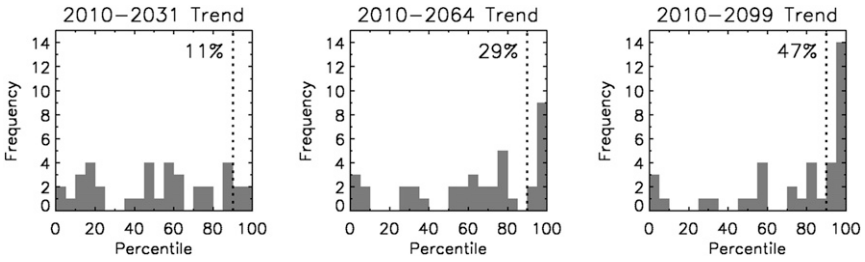

FIG. 7. Histograms of the percentile at which each model's projected trend lies within its distribution of unforced trends. Trends are of GHAfrica MAM average rainfall for (left) 2010–31, (center) 2010–64, and (right) 2010–99. Each model contributes a single percentile to each histogram, and unforced trends are derived from the same model's preindustrial control integration and are of the same length as the projected trend. The values at the top right of each panel record the percentage of models for which the projected trend lies beyond the 90th percentile.

unprecedented in its persistence and intensity from at least circa 1874, although its bidecadal downward trend is exceeded by one other period.

Hence, we have a second line of evidence (alongside that of section 5a) that if the recent long rains droughts were solely due to natural climate variability, then it was probably a rather unusual natural event. Alternatively, and more likely, these droughts either arose from changing anthropogenic forcing (such as CO_2, aerosols, etc.) or from a combination of anthropogenic and natural drivers [such as noted by Liebmann et al. (2014), or involving the aerosol or land-use forcing discussed in sections 6 and 7]. Further work is now required to attribute the long rains trend to specific SST drivers and, then, to attribute these relevant SSTs to natural and/or anthropogenic forcing. Section 9 will place these ideas into the context of our evaluation of other hypotheses.

c. *Natural decadal variability in future projections*

We now assess the extent to which the projected upward trend in the long rains differs from unforced natural decadal variability. The approach is similar to that of section 5a. Each model's projected trend of GHAfrica MAM rainfall (using the RCP8.5 scenario) is compared with the same model's distribution of preindustrial control trends arising only from natural climate variations. Separate calculations are made for 22-, 45-, and 90-yr trends each starting in 2010, and compared with all possible control trends of the same length from the same model. Unlike section 5a, no normalization is required. We compute the percentile of each model's projected trend within its distribution of control trends to determine whether its projection is beyond the range due to natural processes. This provides 42 percentiles for each of the three trend lengths; the distributions of which are shown in Fig. 7.

Short-period projections of MAM rainfall trends (22 years ahead) do not differ significantly from natural climate variability, with only 10% of models lying beyond the 90th percentile (Fig. 7, left). On the other hand, long-period trends (to the end of the twenty-first century) are beyond the range of natural variability in almost half the CMIP5 models (Fig. 7, right), and are positive but weaker in another 32% of models, also implying increased likelihood of an above-average wet season. At intermediate time scales, 45 years ahead, a quarter of the model projections have an upward trend beyond the naturally occurring range (Fig. 7, center). Furthermore, if we assume that the response to anthropogenic forcing is linear with time (verified in section 8), then the models with increased risk of wet extremes after 90 years must also have increased risk (albeit a smaller risk) of wet extremes after 45 years (unless a changing balance between different forcings invalidates this assumption; recall hypotheses D and E).

It is also worthwhile quantifying the relative roles of natural variability and modeling uncertainty in the projections of GHAfrica MAM rainfall anomalies. This can be estimated following the methodology of Rowell (2012). Thus, the variance of projected-minus-control anomalies $\sigma^2_{\Delta P\_Total}$ is separated into a component due to natural variability $\sigma^2_{\Delta P\_Nat}$ [details follow AO-PPE-A in appendix 2 of Rowell (2012)], and a component due to uncertainty in the model formulation $\sigma^2_{\Delta P\_Model}$. These calculations reveal that by the end of the twenty-first century the role of natural variability is insubstantial compared to modeling uncertainty, whereby $\sigma^2_{\Delta P\_Model}/\sigma^2_{\Delta P\_Nat} = 9.9$ in the case of 2070–99 GHAfrica average anomalies. Nevertheless, natural variability inevitably plays a larger role for smaller regions, or for shorter periods or earlier periods. For example, for the 2035–64 or 2015–44 GHAfrica average anomalies, $\sigma^2_{\Delta P\_Model}/\sigma^2_{\Delta P\_Nat} = 4.2$ or 2.6, respectively.

A corollary of this dominance of modeling uncertainty is that if its key drivers can be understood and used to develop observational constraints on model spread, then there is the potential to significantly reduce the total uncertainty in projected rainfall anomalies over East Africa.

6. Aerosol emissions (hypothesis D)

Here, we address the hypothesis that the recent downward trend in the East African long rains is due to changes in anthropogenic aerosol emissions. Evidence for an aerosol influence on rainfall trends has been presented for the Sahel (e.g., Ackerley et al. 2011), South Asia (Bollasina et al. 2011), the Amazon (Cox et al. 2008), and the Pacific (Allen et al. 2014; Boo et al. 2015). Perhaps most studied has been the Sahel, where a number of papers have shown that the 1950–80 downward trend was partly due to the substantial rise in aerosol loading from European and North American emissions, via changes in North Atlantic SSTs (e.g., Williams et al. 2001; Held et al. 2005; Kawase et al. 2010; Ackerley et al. 2011). It thus seems plausible that the recent rapid increase in Asian aerosol emissions (Shindell et al. 2013), or perhaps the decline in European and North American emissions, might be a potential driver of the evolution of the East African long rains. Whether or not this has been the case depends on the pattern and magnitude of the aerosol-driven radiative forcing anomalies across the tropical Indo-Pacific and whether this projects onto the anomalous SST patterns that drive the decadal variability of the long rains.

This possibility can be assessed through the analysis of model sensitivity experiments that include or exclude anthropogenic aerosol emissions. Such experiments are available from the CMIP5 archive. Three models—CSIRO Mk3.6.0, HadGEM2-ES, and IPSL-CM5A-LR—were rerun for an ensemble of 1850–2005 historical experiments but instead used anthropogenic aerosol emissions fixed at preindustrial values (note that the HadGEM2-ES experiment is not available from CMIP5). These are labeled as NoAA experiments. By computing their ensemble mean 1986–2005 trend of rainfall and SSTs, and subtracting this from the mean of the corresponding ensemble members in the standard historical experiment, the magnitude of the aerosol impact on these trends can be assessed. A further five models—CanESM2, CCSM4, CSIRO Mk3.6.0, GFDL CM3, and GISS-E2-R—ran an ensemble of historical integrations in which estimates of historical anthropogenic aerosol emissions were specified but all other anthropogenic and natural forcings were fixed at their preindustrial values. These are labeled as AAOnly experiments. In this case the role of aerosol emissions is evaluated directly from the sensitivity experiment's ensemble mean 1986–2005 trends. For both types of experiment, an average over 3–5 ensemble members is assessed. Single-member experiments of two further models were excluded because individual members of the available ensembles show considerable divergence as a result of chaotic variations in the coupled ocean–atmosphere system.

Figure 8 illustrates the modeled role of anthropogenic aerosol emissions on recent MAM rainfall trends over Africa. Local statistical significance is computed using a Monte Carlo approach to test the null hypothesis that these trends are entirely due to unforced natural climate variability. Several 20-yr periods, completely separated by at least 10 years are randomly selected from each model's control experiment, then averaged into two independent ensemble means (of the same size as the model's sensitivity experiment), and then the difference between their trends is computed. This is repeated 1000 times to provide a reference distribution of unforced trends (1000 is shown to be sufficient to provide robust results). If the historical-minus-NoAA trend lies beyond the 5th or 95th percentiles of this distribution, then the null hypothesis is rejected at the 10% significance level. Similarly the AAOnly trends are compared against a distribution of 1000 randomly selected ensemble mean 20-yr control trends. Figure 8 shows that the impact of changes in anthropogenic aerosols on rainfall trends is not statistically significant over more than about 10% of the African continent, and so cannot be considered field significant. In other words, the modeled impact of aerosols on MAM African rainfall is not detectable above the noise of natural climate variations.

However, we know that the recent rainfall trend is at least partly driven by anomalous SSTs (section 4), and we also know that modeled SST–rainfall teleconnections tend to be too weak for Africa (Rowell 2013). It is possible therefore that the hypothesis of this section remains valid, but that the models fail to transmit an aerosol signal from altered SSTs to altered African rainfall. This possibility is also heightened by the fact that observed SST teleconnections to the long rains are known to be weaker than other SST–rainfall teleconnections (e.g., Ogallo et al. 1988; Nicholson 1996; Hastenrath et al. 2011). Thus, in Fig. 9 we also show the modeled sensitivity of 1986–2005 SST trends to evolving anthropogenic aerosol emissions alone. This follows Dong and Zhou's (2014) analysis of the Indian Ocean, but here addresses the entire tropics, since the Pacific may have driven the long rains trend (section 4; Lyon and DeWitt 2012). Statistical significance is computed using the same Monte Carlo approach as described above, except that the average tropical trend (30°N–30°S) is subtracted from all computed trend patterns, because our interest is in the significance of the pattern of SST response not the global cooling tendency due to enhanced aerosol loading (this adjustment is applied for statistical testing alone, and not to alter the colored values shown in Fig. 9).

Two models display a field significant pattern of SST response to changing aerosol emissions over this period, whereas others have no field significant SST pattern response (Fig. 9). For two of these latter models, their weak

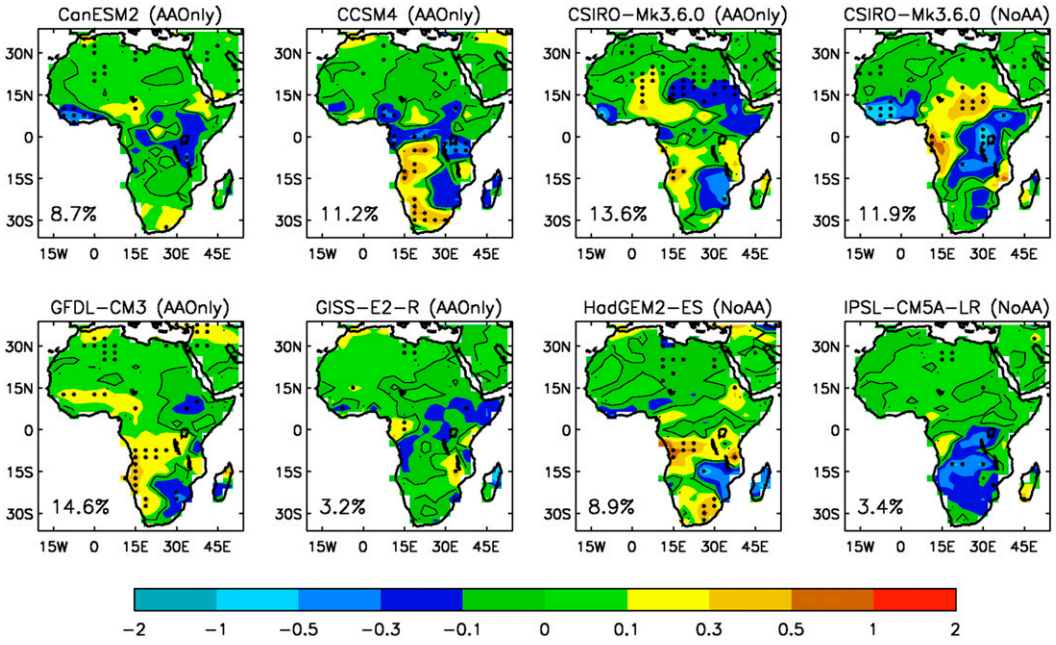

FIG. 8. Impact of anthropogenic aerosol emissions on 1986–2005 MAM rainfall trends (mm day^{-1} decade^{-1}). Black dots show the local rejection of a null hypothesis of no impact on trend at the 10% significance level, with the areal percentage of such points shown in the bottom-left corner of each panel.

SST response may be due to structural limitations in their modeling: a lack of representation of aerosol–cloud interactions in CCSM4 and an offline computation of the relationship between cloud brightness and aerosols in IPSL-CM5A-LR. The five remaining models are more structurally complete in their representation of the radiative effects of aerosols, but still suggest a lack of consensus as to whether, or how, tropical SST patterns responded to changing aerosol emissions from 1986 to 2005. CanESM2, HadGEM2-ES, and GISS-E2-R again fail to achieve field significance, suggesting that the modeled impact of aerosols on African rainfall is not detectable above the noise of natural climate variations. In contrast, the results of the CSIRO Mk3.6.0 NoAA and GFDL CM3 AAOnly experiments do appear to be field significant, but their patterns of aerosol response differ substantially from each other. CSIRO Mk3.6.0 suggests that aerosol forcing during this period led to cooling throughout the tropical Indo-Pacific basin, peaking in the western Indian Ocean, the western equatorial Pacific, and the southeastern tropical Pacific. GFDL CM3 suggests that the strongest effect was a cooling close to the equator, with the exception of warming in the equatorial western Pacific. It is possible that either of these patterns of recent trends could have had a more substantive impact on East African climate than the warming trends over the same period. Note that the largest spatial correlation between panels in Fig. 9 is between the two CSIRO Mk3.6.0 experiments, suggesting the approximate linearity to the inclusion or exclusion of anthropogenic aerosol forcing, although the low magnitude of this correlation (0.51) emphasizes the large role of natural variability in bidecadal trends.

Thus, models suggest considerable uncertainty as to whether or not anthropogenic aerosol emissions might have played a role in the 1986–2005 evolution of tropical Pacific and Indian Ocean SST patterns, and so likewise in the decline of the East African long rains. Probable reasons for this uncertain modeling are (i) a possible underestimate of Asian sulfate aerosol emissions in the RCP scenarios [e.g., Lu et al. (2011) illustrate post-2006 differences between declining inventory-based estimates of SO_2 emissions and recent satellite products that show little decline], (ii) uncertainties in aerosol emissions from biomass burning (Bond et al. 2013), (iii) uncertain modeling of the processes known to determine the radiative forcing response (e.g., Shindell et al. 2013) and the possibility of unknown aerosol-related processes not yet included in models, and (iv) inadequate modeling of teleconnections from SSTs to African rainfall. These shortcomings may also partly explain the wide variety of (and often weak) long rains trends in the CMIP5 historical runs (Fig. 3a). In conclusion, understanding and modeling of the role of changing anthropogenic aerosol emissions is currently inconclusive. We suggest this should remain a candidate driver of the recent downward trend in the East African long rains, to be considered

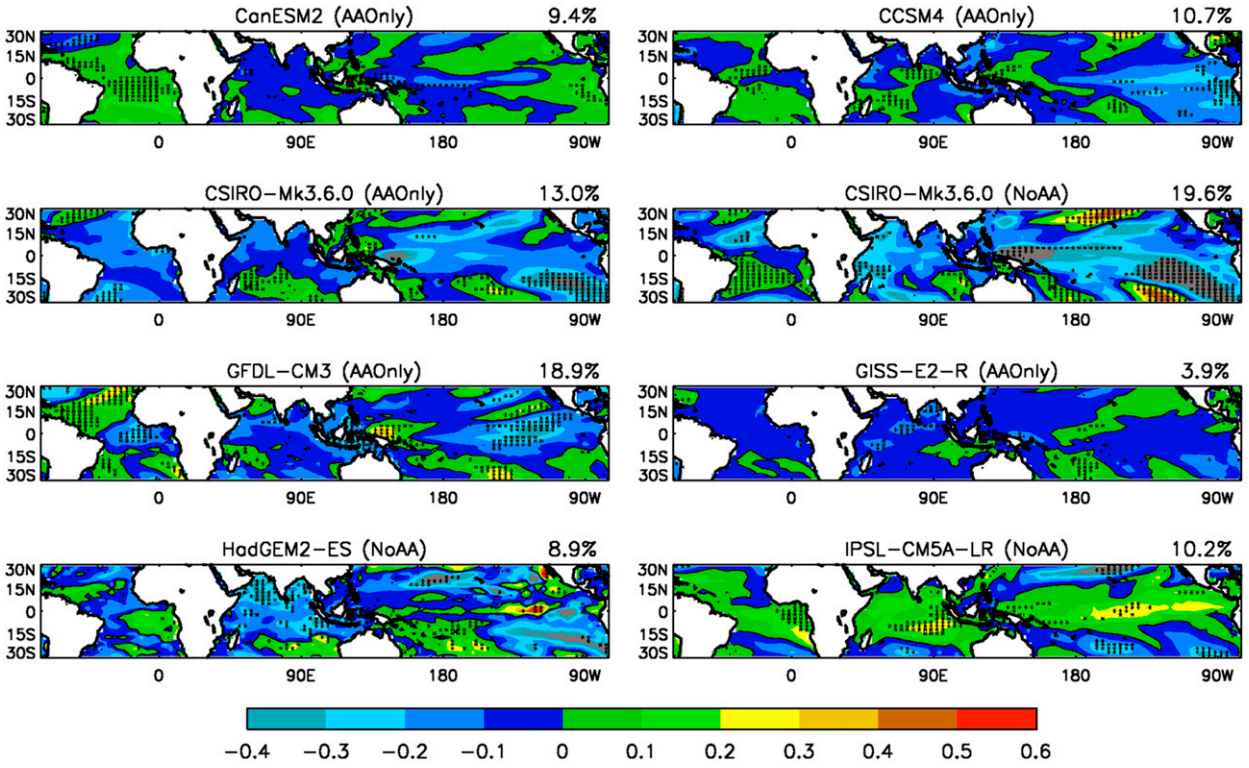

FIG. 9. As in Fig. 8, but for SST trends (°C decade^{-1}), and the percentage of significant points is instead shown on the right above each panel.

within the context of other hypotheses (section 9). Certainly, further research and model development is required to investigate the role of aerosols in the past trend, and also their possible role over the coming decades.

7. Changing land use (hypothesis E)

In this section we address the hypothesis that the recent downward trend in the long rains may be due to land-use change over and around East Africa. A number of studies have shown that tropical climate can be sensitive to large perturbations of the land surface, such as replacing present-day land cover with an estimate of zero anthropogenic influence (Chase et al. 2000) or applying sizeable twenty-first-century increases in crop and pasture land (Hagos et al. 2014). For East Africa, Otieno and Anyah (2012) and R. O. Anyah (2014, personal communication) found a moderate and statistically significant sensitivity of rainfall to a somewhat inflated representation of the recent expansion of Kenyan agriculture in a single-model study. This land-use hypothesis for the recent droughts therefore demands further investigation, employing a multimodel analysis and a scenario for land-use change that is both realistic and global in its extent (i.e., includes plausible surrounding influences such as deforestation in central Africa).

This can again be examined using sensitivity experiments from the CMIP5 archive. Three models (CanESM2, GISS-E2-R, and CCSM4) performed an ensemble of 1850–2005 integrations forced only by observed land-use changes (from Hurtt et al. 2011), with all other forcings held at their preindustrial values. We label these as LUOnly experiments, and ensemble sizes were either three or five members. Other models, which ran similar experiments with only one or two members, were excluded because of the need to enhance the signal-to-noise ratio in the presence of the large chaotic variability of the coupled ocean–atmosphere system (cf. section 6).

The ensemble mean 1986–2004 rainfall trend of these LUOnly experiments is shown in Fig. 10 (note that one member of the CCSM4 experiment ends prematurely in 2004, thus shortening the end of the trend period, but comparison with 1986–2005 trends in the other models shows no sensitivity to this small difference). Local statistical significance was computed following the Monte Carlo approach described in section 6. Only one grid box within the GHAfrica region is statistically significant, and Africa as a whole fails to achieve field significance. Thus, the modeled impact of changing land use on MAM African rainfall is not detectable for this particular period above the noise of natural climate variations.

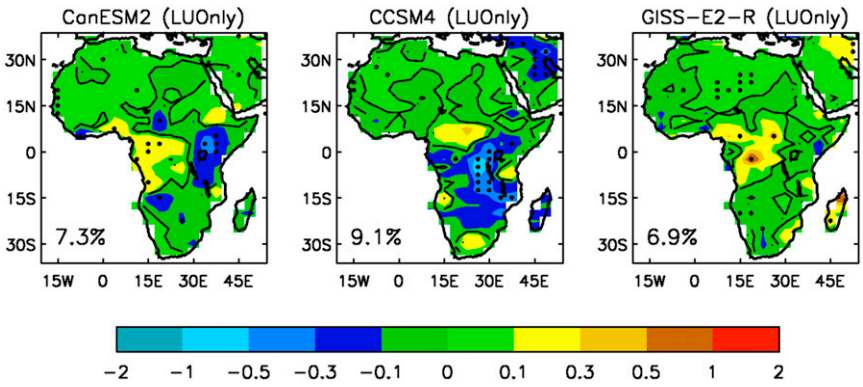

FIG. 10. As in Fig. 8, but for the impact of land-use changes on 1986–2004 MAM rainfall trends.

Consideration might also be given to a complementary analysis of AGCM experiments (to eliminate the component of noise due to SST variations in coupled models), to an independent assessment of the realism of the Hurtt et al. (2011) land-use scenario over East Africa, and to the potential contribution of known deficiencies in the modeling of land–atmosphere coupling. However, we suggest that these topics should be of lower priority since not even a weak signal is found here. On the other hand, it can be anticipated that land-use change might become more important over the coming decades, because of rapid urban growth, particularly in the Lake Victoria basin (Seto et al. 2012; F. H. M. Semazzi 2014, personal communication), and perhaps also because of deforestation in the Congo basin.

8. Nonlinear WMGHG impacts (hypothesis F)

Here, we address the hypothesis that the contrast between the past and future long rains trends is due to a nonlinear evolution of WMGHG impacts. This could be because the balance between competing mechanistic responses is changing, or because one or more mechanism responds nonlinearly. Thorpe and Andrews (2014) show a nonlinear evolution of global-mean precipitation, because of a twentieth-century cancelation between the positive effect of surface warming and the negative effect of direct tropospheric radiative forcing, followed by larger twenty-first-century growth in the surface warming effect. Chadwick and Good (2013) investigate substantial regional variations in this nonlinearity, focusing on annual mean marine precipitation, and Hawkins et al. (2014) illustrate a long-term (to 2300) nonlinearity over South America. Perhaps these effects (partly) explain the observed-to-projected change in the direction of the long rains trend if another mechanism also drives an additional underlying long-term downward trend.

To address this possibility, we look at the stabilization period (2100–99) of the RCP8.5 and RCP4.5 scenarios that are available from eight models. These each provide 100 years of data during which the forcing is fixed at either of two rather different levels, leading to good signal-to-noise ratios. To detect nonlinearity we look for evidence that the RCP8.5-minus-RCP4.5 GHAfrica rainfall anomaly is notably larger (or smaller) than the RCP4.5-minus-control anomaly. Both rainfall anomalies are scaled by the associated global mean annual mean temperature anomaly to account for the different forcing anomalies. If anthropogenic impacts evolve linearly, then the difference between these scaled anomalies—the data plotted in Fig. 11—will be zero. This calculation is stratified by month, and statistical significance is assessed using Student's *t* test.

Figure 11 compares this assessment of the long-term nonlinearity of GHAfrica rainfall with the contrast between the past and future GHAfrica rainfall trends. The latter is computed in Fig. 11a as the difference between the ensemble mean 2010–98 RCP8.5 rainfall trend and the observed 1986–2007 rainfall trend (averaged over seven datasets), both scaled by their corresponding global mean annual mean temperature trends. This simulation has the same units as the remaining panels in Fig. 11. It is therefore apparent that nonlinear mechanistic responses to WMGHG forcing explain no more than 10% of the recent contrast in trends[4] (note that Fig. 11a has a scale that differs from the other panels). As an aside, the "sign" of this small nonlinearity is also uncertain during the long rains (see the differences between the minority of models that demonstrate significant MAM nonlinearity),

[4] Note that in the RCP scenarios, aerosol emissions are approximately proportional to CO_2 emissions, so the former are unlikely to be an important driver of nonlinear regional responses during the stabilization period of these projections. Furthermore, results similar to those in Fig. 11h are obtained by analyzing HadGEM2-ES experiments in which only the CO_2 forcing is altered ($1 \times CO_2$, $2 \times CO_2$, and $4 \times CO_2$; not shown).

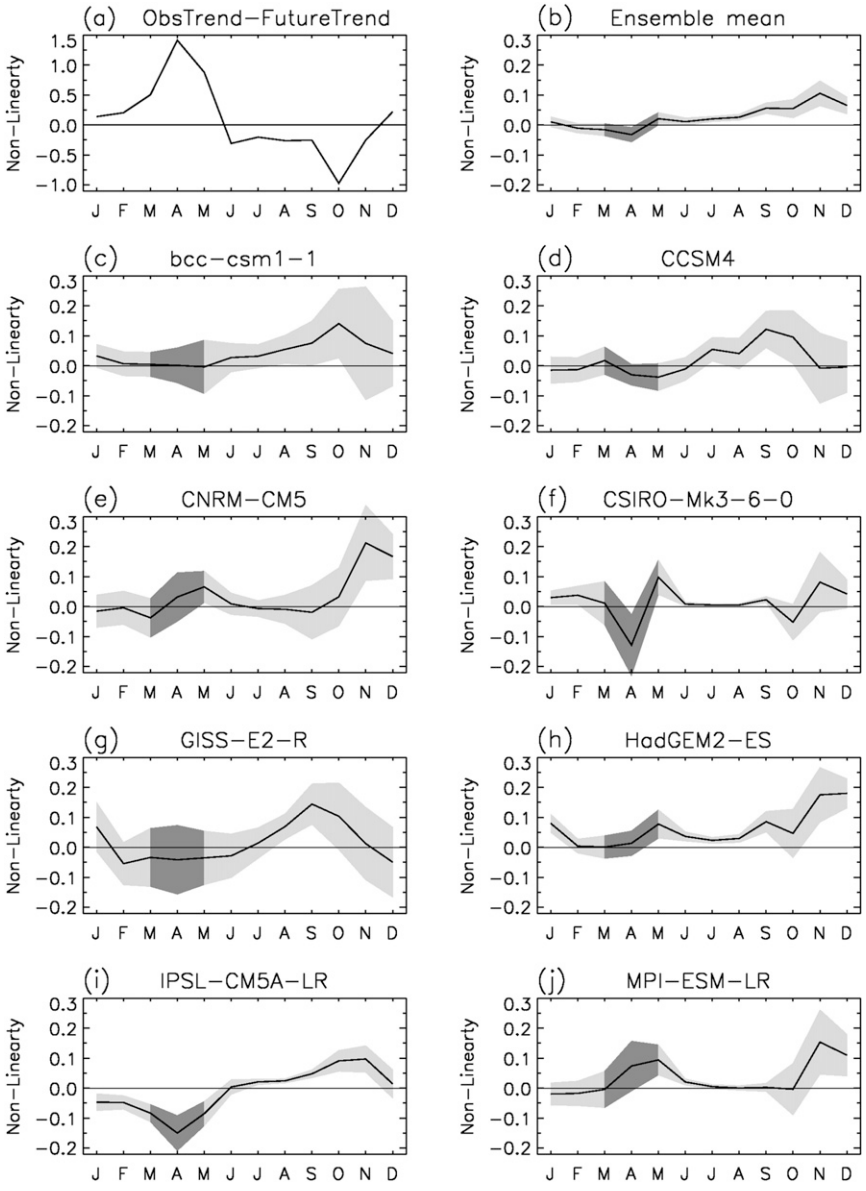

FIG. 11. Nonlinearity metric (see section 8) of the evolution of GHAfrica rainfall. (a) Nonlinearity from the 1986–2007 observed trend to the CMIP5 ensemble mean 2010–98 projected trend. (b)–(j) The 100-yr averages of the nonlinearity from the CMIP5 control experiment to 2100–99 in the RCP4.5 projection to 2100–99 in the RCP8.5 projection. Ensemble mean data in (b) use the eight individual models shown in (c)–(j). Shading in (b)–(j) is the 90% confidence interval, with darker gray shading highlighting the MAM long rains.

but is more consistent during the short rains with a slightly larger proportionate rainfall increase as the forcing grows.

9. Conclusions

The "long rains" season of the greater Horn of Africa has experienced declining rainfall over the past two to three decades, with a series of recent droughts bringing much hardship and loss of life. In contrast, climate model projections suggest an increase in rainfall, especially during March and April (as well as November–February), although their results are not unanimous. We have addressed this East African climate paradox by stepping back and using a logical framework to list all underlying hypotheses that may conceivably resolve it, without preconception as to their likelihood. Recognizing that substantial resources and much literature will be required to properly resolve this paradox, we have

provided an overview across these hypotheses (with the important exception of hypothesis B; see below). We have assessed and synthesized key data relevant to each hypothesis, to begin to understand their likelihood within the context of the other hypotheses, and so recommend priorities for further research.

Hypothesis A was that the recent downward trend of rainfall could be an artifact of poor quality data. This was easily discounted on the basis that there is already good evidence for a long rains decline over the past two to three decades. Observational analysis presented here, using seven gridded datasets and a gauge average dataset, was also unanimous in this regard. Nevertheless, a better understanding of the weaker decline of the CRU dataset would be helpful, particularly for judging the role of natural variability with greater assurance.

Hypothesis B suggests that the projected trends might be founded on the models' poor representation of some key physical processes, and so cannot be trusted. This was not assessed here because we believe there are no shortcuts toward forming even an initial judgment of its likelihood. Rather, a thorough understanding of the mechanisms of projected model change over East Africa is required, leading to an understanding of the key processes that drive uncertainty and an expert judgment of the overall reliability of the CMIP projections. It is also unclear whether the processes that drive uncertainty in future projections are closely linked to those that induce errors in the models' representation of past climate, such as those detailed by Williams and Funk (2011), Otieno and Anyah (2013a), and Yang et al. (2014). Further research must therefore include a thorough understanding of the links between past and future modeling uncertainty. If it seems unlikely that strong systemic biases affect all of the models' projections, then further research could develop observational constraints to reduce the weighting of some models and potentially reduce uncertainty. Kent et al. (2015) have begun this approach by showing that the thermodynamic moisture increase dominates the tendency for a wetter long rains season in a warmer world, whereas uncertain spatial shifts in convection drive much of the intermodel spread in rainfall change. Within the context of the other hypotheses, the present study has not strongly confirmed any of the alternatives to hypothesis B (which would infer the latter is unlikely), nor has it refuted all alternatives (which would infer hypothesis B is valid). Thus, an important research priority is to now undertake a series of thorough investigations that will either place our instinctive faith in CMIP5's projections on a firmer foundation, or clearly demonstrate that the change mechanisms in the current generation of models are erroneous.

Hypothesis C was that the past and/or future trends might arise from natural variability, either on interannual or multidecadal time scales. Two independent lines of evidence, examined in section 5, suggest that natural climate variability is perhaps unlikely to have been the only driver of the recent droughts. Nevertheless, an exceptional natural event cannot be ruled out. Furthermore, a contributing role of natural variability—coincident with that of another driver, such as aerosol forcing—remains a possibility. Caveats are that our analysis (i) is reliant on the capability of climate models to adequately represent the relevant unforced multidecadal modes, (ii) is sensitive to the validity of the CRU trends, and (iii) depends on the limited time span of the East African rain gauge network. In any case, natural variability plays an important role, particularly at shorter time scales such as two decades or less. Looking to the future, even if modeling uncertainty can be substantially reduced, a risk-based prediction approach will always be required, particularly at smaller spatiotemporal scales. Further work must now improve our understanding of the mechanisms of natural variability over GHAfrica, using both model and observed data. This should include poorly understood foundational issues such as the prominent seasonal cycle in the strength of SST–rainfall relationships, an attribution of the recent SST evolution to natural versus anthropogenic sources, and sensitivity experiments that address the relative impact of these attributed SSTs on East Africa.

The remaining hypotheses suggest that there could be genuine physical reasons for the contrast in trends. One possibility is that the balance between competing forcings could be changing, with the past trend driven more by either anthropogenic aerosol emissions or land-use changes and the projected trend driven more by carbon emissions.

Thus, hypothesis D proposed that the downward trend of the long rains may be due to changing anthropogenic aerosol emissions. Evidence from CMIP5 sensitivity experiments was found to be mixed. Models with more sophisticated representations of aerosol–climate interactions were divided between those with an undetectable SST response and those with a significant but uncertain response of the pattern of tropical Indo-Pacific MAM 1986–2005 SST trends. If the latter occurred in reality, then such a pattern of SST trends could in turn have affected East Africa. However, the simulated sensitivity of GHAfrica MAM rainfall trends was insignificant in all models for 1986–2005, although there is reason to believe that this may be due to inadequate modeling of SST–rainfall teleconnections. Thus, considerable uncertainty remains about the role of

anthropogenic aerosol emissions in the recent long rains droughts. Given our analysis revealed no other well-evidenced driver for these droughts, aerosol emissions must remain a candidate hypothesis, either in isolation or alongside other drivers such as natural variability. The scientific community should now focus on improving the modeling of aerosol–climate interactions and SST–rainfall teleconnections, and reassess the reliability of the historic aerosol emissions scenario used in CMIP simulations. Furthermore, predictions of the future climate of East Africa also require robust insights as to whether aerosol-driven radiative forcing anomalies project onto the SST patterns that drive GHAfrica decadal variability. If they do, then the shaping of worldwide national air quality policies, which determine anthropogenic aerosol emissions, represents a key uncertainty in medium-term climate prediction for the region. In particular, if hypothesis D is valid, these policies could also determine when the long rains droughts turn to more abundant rainfall and more frequent flooding.

Hypothesis E was that the recent rainfall trend could have been driven by land-use changes over and beyond East Africa. Model sensitivity experiments showed no detectable impact of the CMIP5 historic land-use scenario on GHAfrica MAM 1986–2004 rainfall trends. Thus, in the absence of evidence that the CMIP5 scenario is grossly underestimated, or that the models' response is consistently grossly underestimated, we suggest that further investigation of this candidate driver of recent droughts should be of lower priority.

Last, hypothesis F suggested that there could be a nonlinear mechanistic response to the dominant anthropogenic forcing. The stabilization period of the CMIP5 RCP4.5 and RCP8.5 projections provides good signal-to-noise ratios, and analysis found that only a minority of models display significant nonlinearity for at least part of the long rains season. The magnitude and seasonality of this nonlinearity varies between models, but crucially explains no more than 10% of the contrast between the recent observed trend and the CMIP5 long-term projected trend. We therefore suggest that further investigation of this candidate driver of the East African paradox should be of low priority.

In conclusion, we believe the research avenues that should now be of highest priority are (i) the development of a process-based expert judgment of the reliability of GHAfrica projections, (ii) further investigation of the idea that changes in anthropogenic aerosol emissions may have driven the recent long rains decline, and (iii) the role of natural variability in the recent droughts. Regarding the future climate, further lines to consider are the potential roles of aerosol emissions and local land-use change.

Acknowledgments. DPR was funded by the U.K. Department for International Development (DFID) for the benefit of developing countries (the views expressed here are not necessarily those of DFID), BBBB and PG were supported by the Joint U.K. DECC–Defra Met Office Hadley Centre Climate Programme (GA01101), and SEN acknowledges the support of NSF Grant 1160750. The many modeling groups listed in Table 1 are gratefully acknowledged for producing and making their simulations available, as is the World Climate Research Programme Working Group on Coupled Modelling (WCRP-WGCM), for taking responsibility for the CMIP5 model archive, and the U.S. Department of Energy's Program for Climate Model Diagnosis and Intercomparison (PCMDI) for archiving the model output. We are also very grateful to Ian Harris for providing the interim "mozfix" version of the CRU data, to Doug Klotter for programming support for SEN, to Laura Wilcox for collating and documenting the "single forcing" experiments submitted to the "historicalMisc" component of CMIP5, to Paul Halloran for running the HadGEM2-ES aerosol sensitivity experiments, and to Richard Graham for discussion of the results.

REFERENCES

Ackerley, D., B. B. B. Booth, S. H. E. Knight, E. J. Highwood, D. J. Frame, M. R. Allen, and D. P. Rowell, 2011: Sensitivity of twentieth-century Sahel rainfall to sulfate aerosol and CO_2 forcing. *J. Climate*, **24**, 4999–5014, doi:10.1175/JCLI-D-11-00019.1.

Adler, R. F., and Coauthors, 2003a: The Version-2 Global Precipitation Climatology Project (GPCP) monthly precipitation analysis (1979–present). *J. Hydrometeor.*, **4**, 1147–1167, doi:10.1175/1525-7541(2003)004<1147:TVGPCP>2.0.CO;2.

——, and Coauthors, 2003b: GPCP2.2: Global Precipitation Climatology Project version 2.2. NASA Goddard Space Flight Center. [Available online at http://precip.gsfc.nasa.gov/gpcp_v2.2_comb_new.html.]

Allen, R. J., J. R. Norris, and M. Kovilakam, 2014: Influence of anthropogenic aerosols and the Pacific decadal oscillation on tropical belt width. *Nat. Geosci.*, **7**, 270–274, doi:10.1038/ngeo2091.

Bollasina, M. A., Y. Ming, and V. Ramaswamy, 2011: Anthropogenic aerosols and the weakening of the South Asian summer monsoon. *Science*, **334**, 502–505, doi:10.1126/science.1204994.

Bond, T. C., and Coauthors, 2013: Bounding the role of black carbon in the climate system: A scientific assessment. *J. Geophys. Res. Atmos.*, **118**, 5380–5552, doi:10.1002/jgrd.50171.

Boo, K.-O., B. B. B. Booth, Y.-H. Byun, J. Lee, C. H. Cho, S. B. Shim, and K.-T. Kim, 2015: Influence of aerosols in multi-decadal SST variability simulations over the North Pacific. *J. Geophys. Res. Atmos.*, **120**, 517–531, doi:10.1002/2014JD021933.

Camberlin, P., and N. Philippon, 2002: The East African March–May rainy season: Associated atmospheric dynamics and predictability over the 1968–97 period. *J. Climate*, **15**, 1002–1019, doi:10.1175/1520-0442(2002)015<1002:TEAMMR>2.0.CO;2.

Chadwick, R., and P. Good, 2013: Understanding nonlinear tropical precipitation responses to CO_2 forcing. *Geophys. Res. Lett.*, **40**, 4911–4915, doi:10.1002/grl.50932.

Chase, T. N., R. A. Pielke Sr., T. G. F. Kittel, R. R. Nemani, and S. W. Running, 2000: Simulated impacts of historical land cover changes on global climate in northern winter. *Climate Dyn.*, **16**, 93–105, doi:10.1007/s003820050007.

CMIP5 Modelling Groups, 2011: Coupled Model Intercomparison Project 5 (with subsequent updates). World Climate Research Programme's Working Group on Coupled Modelling, Earth System Grid Federation, accessed January 2014. [Available online at https://pcmdi9.llnl.gov/projects/cmip5/.]

Cox, P. M., and Coauthors, 2008: Increasing risk of Amazonian drought due to decreasing aerosol pollution. *Nature*, **453**, 212–215, doi:10.1038/nature06960.

Dong, L., and T. Zhou, 2014: The Indian Ocean sea surface temperature warming simulated by CMIP5 models during the twentieth century: Competing forcing roles of GHGs and anthropogenic aerosols. *J. Climate*, **27**, 3348–3362, doi:10.1175/JCLI-D-13-00396.1.

Friedlingstein, P., and Coauthors, 2014: Persistent growth of CO_2 emissions and implications for reaching climate targets. *Nat. Geosci.*, **7**, 709–715, doi:10.1038/ngeo2248.

Gao, C. C., A. Robock, and C. Ammann, 2008: Volcanic forcing of climate over the past 1500 years: An improved ice core-based index for climate models. *J. Geophys. Res.*, **113**, D23111, doi:10.1029/2008JD010239.

Hagos, S., L. R. Leung, Y. Xue, A. Boone, F. de Sales, N. Neupane, M. Huang, and J.-H. Yoon, 2014: Assessment of uncertainties in the response of the African monsoon precipitation to land use change simulated by a regional model. *Climate Dyn.*, **43**, 2765–2775, doi:10.1007/s00382-014-2092-x.

Harris, I., P. D. Jones, T. J. Osborn, and D. H. Lister, 2014: Updated high-resolution grids of monthly climatic observations—The CRU TS3.10 dataset. *Int. J. Climatol.*, **34**, 623–642, doi:10.1002/joc.3711.

Hastenrath, S., D. Polzin, and C. Mutai, 2011: Circulation mechanisms of Kenya rainfall anomalies. *J. Climate*, **24**, 404–412, doi:10.1175/2010JCLI3599.1.

Hawkins, E., M. Joshi, and D. Frame, 2014: Wetter then drier in some tropical areas. *Nat. Climate Change*, **4**, 646–647, doi:10.1038/nclimate2299.

Held, I. M., T. L. Delworth, J. Lu, K. L. Findell, and T. R. Knutson, 2005: Simulation of Sahel drought in the 20th and 21st centuries. *Proc. Natl. Acad. Sci. USA*, **102**, 17 891–17 896, doi:10.1073/pnas.0509057102.

Hillbruner, C., and G. Moloney, 2012: When early warning is not enough—Lessons learned from the 2011 Somalia famine. *Global Food Secur.*, **1**, 20–28, doi:10.1016/j.gfs.2012.08.001.

Hoell, A., and C. Funk, 2013: The ENSO-related West Pacific sea surface temperature gradient. *J. Climate*, **26**, 9545–9562, doi:10.1175/JCLI-D-12-00344.1.

——, and ——, 2014: Indo-Pacific sea surface temperature influences on failed consecutive rainy seasons over eastern Africa. *Climate Dyn.*, **43**, 1645–1660, doi:10.1007/s00382-013-1991-6.

Hurtt, G. C., and Coauthors, 2011: Harmonization of land-use scenarios for the period 1500–2100: 600 years of global gridded annual land-use transitions, wood harvest, and resulting secondary lands. *Climatic Change*, **109**, 117–161, doi:10.1007/s10584-011-0153-2.

Janowiak, J. E., and P. Xie, 1999a: CAMS-OPI: A global satellite–rain gauge merged product for real-time precipitation monitoring applications. *J. Climate*, **12**, 3335–3342, doi:10.1175/1520-0442(1999)012<3335:COAGSR>2.0.CO;2.

——, and ——, 1999b: CAMS-OPI: Climate Anomaly Monitoring System outgoing longwave radiation precipitation index. NOAA/National Weather Service/Climate Prediction Center. [Available online at http://www.cpc.ncep.noaa.gov/products/global_precip/html/wpage.cams_opi.html.]

Kawase, H., M. Abe, Y. Yamada, T. Takemura, T. Yokohata, and T. Nozawa, 2010: Physical mechanism of long-term drying trend over tropical North Africa. *Geophys. Res. Lett.*, **37**, L09706, doi:10.1029/2010GL043038.

Kent, C., R. Chadwick, and D. P. Rowell, 2015: Understanding uncertainties in future projections of seasonal tropical precipitation. *J. Climate*, **28**, 4390–4413, doi:10.1175/JCLI-D-14-00613.1.

Liebmann, B., and Coauthors, 2014: Understanding recent eastern Horn of Africa rainfall variability and change. *J. Climate*, **27**, 8630–8645, doi:10.1175/JCLI-D-13-00714.1.

Lott, F. C., N. Christidis, and P. A. Stott, 2013: Can the 2011 East African drought be attributed to human-induced climate change? *Geophys. Res. Lett.*, **40**, 1177–1181, doi:10.1002/grl.50235.

Lu, Z., Q. Zhang, and D. G. And Streets, 2011: Sulfur dioxide and primary carbonaceous aerosol emissions in China and India, 1996–2010. *Atmos. Chem. Phys.*, **11**, 9839–9864, doi:10.5194/acp-11-9839-2011.

Lyon, B., 2014: Seasonal drought in the greater Horn of Africa and its recent increase during the March–May long rains. *J. Climate*, **27**, 7953–7975, doi:10.1175/JCLI-D-13-00459.1.

——, and D. G. DeWitt, 2012: A recent and abrupt decline in the East African long rains. *Geophys. Res. Lett.*, **39**, L02702, doi:10.1029/2011GL050337.

Mason, J. B., J. M. White, L. Heron, J. Carter, C. Wilkinson, and P. Spiegel, 2012: Child acute malnutrition and mortality in populations affected by displacement in the Horn of Africa, 1997–2009. *Int. J. Environ. Res. Public Health*, **9**, 791–806, doi:10.3390/ijerph9030791.

Matsuura, K., and C. J. Willmott, 2009: Terrestrial precipitation: 1900–2008 gridded monthly time series (version 2.01). Center for Climatic Research, University of Delaware. [Available online at http://climate.geog.udel.edu/~climate/html_pages/Global2_Ts_2009/README.global_p_ts_2009.html.]

Nicholson, S. E., 1996: A review of climate dynamics and climate variability in eastern Africa. *The Limnology, Climatology and Paleoclimatology of the East African Lakes*, T. C. Johnson and E. Odada, Eds., Gordon and Breach, 25–56.

——, 2000: The nature of rainfall variability over Africa on time scales of decades to millennia. *Global Planet. Change*, **26**, 137–158, doi:10.1016/S0921-8181(00)00040-0.

——, 2014: A detailed look at the recent drought situation in the Greater Horn of Africa. *J. Arid Environ.*, **103**, 71–79, doi:10.1016/j.jaridenv.2013.12.003.

——, 2015: Long-term variability of the East African ''short rains'' and its links to large-scale factors. *Int. J. Climatol.*, **35**, 3979–3990, doi:10.1002/joc.4259.

——, A. K. Dezfuli, and D. Klotter, 2012: A two-century precipitation dataset for the continent of Africa. *Bull. Amer. Meteor. Soc.*, **93**, 1219–1231, doi:10.1175/BAMS-D-11-00212.1.

Ogallo, L. J., J. E. Janowiak, and M. S. Halpert, 1988: Teleconnection between seasonal rainfall over East Africa and global sea surface temperature anomalies. *J. Meteor. Soc. Japan*, **66**, 807–822.

Otieno, V. O., and R. O. Anyah, 2012: Effects of land use changes on climate in the Greater Horn of Africa. *Climate Res.*, **52**, 77–95, doi:10.3354/cr01050.

——, and ——, 2013a: CMIP5 simulated climate conditions of the Greater Horn of Africa (GHA). Part 1: Contemporary climate. *Climate Dyn.*, **41**, 2081–2097, doi:10.1007/s00382-012-1549-z.

——, and ——, 2013b: CMIP5 simulated climate conditions of the Greater Horn of Africa (GHA). Part II: Projected climate. *Climate Dyn.*, **41**, 2099–2113, doi:10.1007/s00382-013-1694-z.

Rayner, N. A., D. E. Parker, E. B. Horton, C. K. Folland, L. V. Alexander, D. P. Rowell, E. C. Kent, and A. Kaplan, 2002: HadISST1.1: Hadley Centre Sea Ice and Sea Surface Temperature version 1.1. Met Office Hadley Centre. [Available online at http://www.metoffice.gov.uk/hadobs/hadisst/.]

——, ——, ——, ——, ——, ——, ——, and ——, 2003: Global analyses of sea surface temperature, sea ice, and night marine air temperature since the late nineteenth century. *J. Geophys. Res.*, **108**, 4407, doi:10.1029/2002JD002670.

Rowell, D. P., 2012: Sources of uncertainty in future changes in local precipitation. *Climate Dyn.*, **39**, 1929–1950, doi:10.1007/s00382-011-1210-2.

——, 2013: Simulating SST teleconnections to Africa: What is the state of the art? *J. Climate*, **26**, 5397–5417, doi:10.1175/JCLI-D-12-00761.1.

Schneider, U., A. Becker, P. Finger, A. Meyer-Christoffer, B. Rudolf, and M. Ziese, 2011: GPCC full data reanalysis version 6 at 1.0°: Monthly land-surface precipitation from rain-gauges built on GTS-based and historic data. NOAA/Earth System Research Laboratory, doi:10.5676/DWD_GPCC/FD_M_V6_100.

——, ——, ——, ——, ——, and ——, 2014: GPCC's new land surface precipitation climatology based on quality-controlled in situ data and its role in quantifying the global water cycle. *Theor. Appl. Climatol.*, **115**, 15–40, doi:10.1007/s00704-013-0860-x.

Seto, K. C., B. Guneralp, and L. R. Hutyra, 2012: Global forecasts of urban expansion to 2030 and direct impacts of biodiversity and carbon pools. *Proc. Natl. Acad. Sci. USA*, **109**, 16 083–16 088, doi:10.1073/pnas.1211658109.

Shindell, D. T., and Coauthors, 2013: Radiative forcing in the ACCMIP historical and future climate simulations. *Atmos. Chem. Phys.*, **13**, 2939–2974, doi:10.5194/acp-13-2939-2013.

Shongwe, M. E., G. J. van Oldenborgh, and B. van den Hurk, 2011: Projected changes in mean and extreme precipitation in Africa under global warming. Part II: East Africa. *J. Climate*, **24**, 3718–3733, doi:10.1175/2010JCLI2883.1.

Tanarhte, M., P. Hadjinicolaou, and J. Lelieveld, 2012: Intercomparison of temperature and precipitation data sets based on observations in the Mediterranean and the Middle East. *J. Geophys. Res.*, **117**, D12102, doi:10.1029/2011JD017293.

Taylor, K. E., R. J. Stouffer, and G. A. Meehl, 2012: An overview of CMIP5 and the experiment design. *Bull. Amer. Meteor. Soc.*, **93**, 485–498, doi:10.1175/BAMS-D-11-00094.1.

Thorpe, L., and T. Andrews, 2014: The physical drivers of historical and 21st century global precipitation changes. *Environ. Res. Lett.*, **9**, doi:10.1088/1748-9326/9/6/064024.

Trenberth, K. E., A. Dai, G. van der Schrier, P. D. Jones, J. Barichivich, K. R. Briffa, and J. Sheffield, 2014: Global warming and changes in drought. *Nat. Climate Change*, **4**, 17–22, doi:10.1038/nclimate2067.

Viste, E., D. Korecha, and A. Sorteberg, 2013: Recent drought and precipitation tendencies in Ethiopia. *Theor. Appl. Climatol.*, **112**, 535–551, doi:10.1007/s00704-012-0746-3.

von Storch, H., and F. W. Zwiers, 1999: *Statistical Analysis in Climate Research.* Cambridge University Press, 484 pp.

Williams, A. P., and C. Funk, 2011: A westward extension of the warm pool leads to a westward extension of the Walker circulation, drying eastern Africa. *Climate Dyn.*, **37**, 2417–2435, doi:10.1007/s00382-010-0984-y.

Williams, K. D., A. Jones, D. L. Roberts, C. A. Senior, and M. J. Woodage, 2001: The response of the climate system to the indirect effects of anthropogenic sulfate aerosol. *Climate Dyn.*, **17**, 845–856, doi:10.1007/s003820100150.

Xie, P., and P. A. Arkin, 1997a: Global precipitation 17-year monthly analysis based on gauge observations, satellite estimates, and numerical model outputs. *Bull. Amer. Meteor. Soc.*, **78**, 2539–2558, doi:10.1175/1520-0477(1997)078<2539:GPAYMA>2.0.CO;2.

——, and ——, 1997b: CMAP: Climate Prediction Center Merged Analysis of Precipitation. NOAA/National Weather Service Climate Prediction Center. [Available online at http://www.cpc.ncep.noaa.gov/products/global_precip/html/wpage.cmap.html.]

Yang, W., R. Seager, and M. A. Cane, 2014: The East African long rains in observations and models. *J. Climate*, **27**, 7185–7202, doi:10.1175/JCLI-D-13-00447.1.